

## **General Disclaimer**

### **One or more of the Following Statements may affect this Document**

- This document has been reproduced from the best copy furnished by the organizational source. It is being released in the interest of making available as much information as possible.
- This document may contain data, which exceeds the sheet parameters. It was furnished in this condition by the organizational source and is the best copy available.
- This document may contain tone-on-tone or color graphs, charts and/or pictures, which have been reproduced in black and white.
- This document is paginated as submitted by the original source.
- Portions of this document are not fully legible due to the historical nature of some of the material. However, it is the best reproduction available from the original submission.

X-660-76-19

PREPRINT

NASA TM X-71052

**ELECTRONS IN A CLOSED GALAXY  
MODEL OF COSMIC RAYS**

**R. RAMATY  
N. J. WESTERGAARD**



**JANUARY 1976**

**GSFC**

**GODDARD SPACE FLIGHT CENTER  
GREENBELT, MARYLAND**

(NASA-TM-X-71052) ELECTRONS IN A CLOSED  
GALAXY MODEL OF COSMIC RAYS (NASA) 35 p HC  
\$4.00 CSCL 03B

N76-18033

Unclassified  
G3/93 14847

# ELECTRONS IN A CLOSED GALAXY MODEL OF COSMIC RAYS

R. Ramaty  
NASA/Goddard Space Flight Center  
Greenbelt, Maryland 20771, USA

and

N. J. Westergaard  
Danish Space Research Institute  
Lyngby, Denmark

## ABSTRACT

We consider the consistency of positrons and electrons with a propagation model in which the cosmic rays are stopped by nuclear collisions or energy losses before they can escape from the galaxy (The closed-galaxy model). The fact that we find no inconsistency between the predictions and the data implies that the protons which produce the positrons by nuclear reactions could have their origin in a large number of distant sources, as opposed to the heavier nuclei which in this model come from a more limited set of sources. The closed-galaxy model predicts steep electron and positron spectra at high energies. None of these are inconsistent with present measurements; but future measurements of the spectrum of high-energy positrons could provide a definite test for the model. The closed-galaxy model also predicts that the interstellar electron intensity below a few GeV is larger than that implied by other models. The consequence of this result is that electron bremsstrahlung is responsible for about 50% of the galactic gamma-ray emission at photon energies greater than 100 MeV.

### 1. Introduction.

Rasmussen and Peters (1975) have recently reexamined the closed-galaxy model for cosmic rays. In this model the cosmic rays are trapped in the Galaxy for times longer than their nuclear destruction times, and an equilibrium is established between production by galactic sources

and losses due to interactions with the interstellar medium. These authors show that the model can explain the observed nuclear composition of cosmic rays provided that the observed cosmic-ray flux near Earth is a superposition of fluxes from a large number of distant sources and from one or perhaps a few local sources.

In the closed-galaxy model cosmic-ray nuclei from distant sources undergo many nuclear interactions leading to secondary nuclei such as Li, Be and B which are not present in the cosmic-ray sources. Since the resultant ratios of secondary-to-primary nuclei from distant sources is much larger than the observed ratios of this kind, it is necessary for the local sources to produce almost all the primary cosmic-ray nuclei with  $Z \geq 2$ . In particular about 90% of the Fe, 80% of the C and O, and 70% of the He have to be local because otherwise the secondary-to-primary ratios resulting from the fragmentation of these nuclei would be larger than observed. (Fragmentation of Fe produces nuclei in the range  $15 \leq Z \leq 25$ , C and O produce Li, Be and B, and  $^4\text{He}$  produces  $^3\text{He}$  and  $^2\text{H}$ ).

Since the majority of cosmic rays consists of protons, it is of considerable interest to determine whether a similar constraint could be placed on protons. This can be done by considering the positron flux in the cosmic rays; the positrons are believed to be secondary products of protons resulting from the decay of  $\pi^+$  mesons which are produced in nuclear interactions of cosmic-ray nuclei with the interstellar gas. Deuterons below several hundreds of MeV are also secondary products of protons, but because they are very strongly affected by solar

modulation (Goldstein, Fisk and Ramaty, 1970; Meyer, 1971), they are not very useful in this study.

In the present paper we calculate the positron flux in the interstellar medium by assuming that a cosmic-ray proton flux equal to that observed near Earth at solar minimum exists everywhere in the confinement volume of the cosmic rays. This assumption allows us to calculate the production rate of positrons and negatrons per gram of interstellar medium, independent of propagation and confinement model. We use previous calculations of Perola, Scarsi and Sironi (1967), Ramaty and Lingefelter (1968), Badhwar et al. (1975) and Orth and Buffington (1976), and we present our results in Section 2.

In Section 3 we evaluate the interstellar positron intensities by taking into account the propagation of these particles and their energy losses. We perform these calculations both in the closed-galaxy model, and in a model in which the cosmic rays escape from the Galaxy (the leaky-box model). The closed-galaxy model yields, in general, larger positron fluxes, but we argue that for a sufficiently low interstellar matter density and a nonvanishing solar modulation up to about 5 GeV, the positron flux in this model is not inconsistent with the available data and the assumption that the proton flux throughout the confinement volume is the same as that measured locally. This result implies that the nearby sources which in the closed-galaxy model are required to produce the bulk of the local primary cosmic rays with  $Z \geq 2$ , need not contribute appreciably to the local proton flux.

In section 4 we evaluate the total interstellar electron flux. From measurements of the positron-to-electron ratio in the cosmic rays

(Fanselow et al., 1969; Daugherty, Hartman and Schmidt, 1975; Buffington, Orth and Smoot, 1975) it is known that the local cosmic electron flux contains primary negatrons in addition to secondary positrons and negatrons. We obtain the total interstellar electron intensity by dividing the calculated positron intensity with the measured  $e^+/e$  ratio. We compare this intensity with the available electron measurements at high energies. We find that, even though the closed-galaxy model yields a steeper electron spectrum than does the leaky box, its predictions are consistent with essentially all the electron data up to energies of several hundred GeV. However, we cannot rule out the possibility that nearby sources could produce the bulk of the observed high-energy electrons ( $\geq 200$  GeV).

In Section 5 we evaluate the gamma-ray emission from electrons in the closed-galaxy model. As a very important modification to accepted ideas, we find that in this model bremsstrahlung from interstellar electrons is a dominant mechanism for the production of galactic gamma rays.

We summarize our conclusions in Section 6.

## 2. Sources of Secondary Electrons.

The principal source of secondary electrons of energies greater than a few tens of MeV are charged  $\pi$  mesons produced in nuclear reactions between cosmic rays and the interstellar medium. Secondary electrons can also be produced by the knock-on process whereby ambient electrons achieve relativistic energies when they collide with cosmic-ray protons and nuclei. Other sources of secondary electrons such as neutrons and

radioactive positron emitters are negligible at energies greater than a few MeV (e.g. Ramaty 1974).

The source functions of interstellar positrons and electrons are independent of the cosmic-ray propagation model. They only depend on the assumed cosmic-ray intensity and the composition of the interstellar medium. We have used the calculations of Ramaty and Lingenfelter (1968) as presented by Ramaty (1974); Perola, Scarsi and Sironi (1967); Abraham, Brunstein and Cline (1966); Orth and Buffington (1976); and Badhwar et al. (1975).

We show the secondary source functions in Figure 1 for an interstellar cosmic-ray intensity which is the same as measured near Earth at solar minimum. Here  $q_+$  and  $q$  are the source functions of positrons and secondary electrons (positrons and negatrons), respectively. Below 1 GeV  $q_+(E)$  and  $q(E)$  are taken from Ramaty (1974). As discussed in this reference, these spectra are in good agreement with the independent calculations of Perola, Scarsi and Sironi (1967). The electron source spectra produced by a solar minimum cosmic-ray intensity are somewhat smaller than those produced by a cosmic-ray intensity which takes into account a finite amount of solar modulation. But because of the relatively high  $\pi$ -meson production threshold energy, a reasonable solar modulation will not increase the electron production by more than a factor of 2 (Ramaty 1974).

The turnup in the total electron spectrum below about 50 MeV is due to the knock-on process. The source function for these electrons is based on the calculations of Abraham, Brunstein and Cline (1966).

Above 1 GeV we plot the quantities  $E^{2.75}q_+$  and  $E^{2.75}q$  taken from a recent calculation of Orth and Buffington (1976). These authors do not present calculations at lower energies. Around 1 GeV, however, there is good agreement between their calculations and the results presented by Ramaty (1974).

An independent calculation of positron production at high energies has also been given by Badhwar et al. (1975), who find that  $E^{2.75}q_+(E) = 3.4 \times 10^{-3} e^+ g^{-1} s^{-1} \text{ GeV}^{1.75}$ . This result, even though not showing the slight flattening of the positron spectrum with respect to the proton spectrum found by Orth and Buffington (1976), is in quite good agreement with the results plotted in Figure 1. In fact, at  $E = 100$  GeV the two calculations give identical results. In the calculations presented in the next sections, we shall use the curves of Figure 1 for  $E < 100$  GeV, and  $E^{2.75}q_+(E) = 3.4 \times 10^{-3}$  and  $E^{2.75}q = 6.4 \times 10^{-3}$  at higher energies. The exponent 2.75 is chosen because the proton spectrum at high energies is proportional to  $E^{-2.75}$  (Ryan et al., 1972).

### 3. Interstellar Positron Intensity.

The propagation of cosmic-ray positrons and negatrons in interstellar space has been discussed in detail in the literature (e.g. Daniel and Stephens 1970, Ramaty 1974). Because only about 10% of the positrons are expected to annihilate at relativistic energies (e.g. Wang and Ramaty 1975), there is no significant difference between the propagation of positrons and negatrons.

In a steady state model with exponential distribution of path lengths (the leaky-box model), the interstellar intensity of positrons can be written as

$$\phi_+(E) = (4\pi dE/dx)^{-1} \int_E^\infty dE' q_+(E') \exp -\int_E^{E'} dE'' (\Lambda dE/dx)^{-1}, \quad (1)$$

where  $q_+$  is the positron source function defined in Section 2;  $dE/dx$  is the positron energy loss per  $\text{g cm}^{-2}$  of interstellar matter; and  $\Lambda$ , measured in  $\text{g cm}^{-2}$ , is the mean path length of the exponential distribution. Both  $\Lambda$  and  $dE/dx$  can be energy dependent.

In the closed-galaxy model,  $\Lambda \rightarrow \infty$  for all  $E$ . Then equation (1) reduces to

$$\phi_+(E) = (4\pi dE/dx)^{-1} \int_E^\infty dE' q_+(E'). \quad (2)$$

The energy loss rate,  $dE/dx$ , consists of ionization, bremsstrahlung, synchrotron and Compton losses. We have taken the ionization and bremsstrahlung losses from Ginzburg and Syrovatskii (1964, equations 8.1, 8.2, 8.3 and 8.5). In neutral and ionized media, the sum of these losses are given by

$$\left(\frac{dE}{dx}\right)_{I+B} = 0.15 [ 3\ln(E/0.51) + 18.8 ] + 0.016E \quad (3)$$

and

$$\left(\frac{dE}{dx}\right)_{I+B} = 0.16[\ln(E/0.51) + 73.4] + 2.85 \times 10^{-3}[\ln(E/0.51) + 0.36] E \quad (4)$$

respectively, where  $dE/dx$  is in  $\text{MeV g}^{-1} \text{cm}^2$  and  $E$  is in MeV.

For the synchrotron losses we have used formula (III-28) of Ramaty (1974) which yields

$$\left(\frac{dE}{dx}\right)_s = 2.1 \times 10^4 (B_\perp^2/n_H) (E/0.51)^2, \quad (5)$$

where, as before,  $dE/dx$  and  $E$  are in  $\text{MeV g}^{-1} \text{cm}^2$  and MeV;  $B_\perp$  is in

gauss; and  $n_H$ , the density of interstellar protons, is in  $\text{cm}^{-3}$ .

Equation (5) is valid for all cosmic-ray electron energies of interest.

For the Compton losses in the Thompson regime we have used formula (III-30) of Ramaty (1974) which is valid for electron energies less than  $(mc^2)^2/\epsilon_r$ , where  $\epsilon_r$  is the mean energy of the ambient photons which scatter the electrons, and  $m$  is the electron mass. The transition energy,  $(mc^2)^2/\epsilon_r$ , is about  $2.5 \times 10^5$  GeV for 3K black-body photons, and  $\sim 80$  GeV for starlight photons. Therefore, the Thompson regime is valid for scattering by 3K black-body photons for all electron energies of interest. For scattering by starlight photons we have to use the Klein-Nishina formula for the Compton cross section. Using the results of Ramaty (1974), we express the total Compton energy loss rate as

$$\left(\frac{dE}{dx}\right)_c = (4.2 \times 10^{-7}/n_H)(E/0.51)^2[W_{bb} + W_v f(E)]. \quad (6)$$

Here  $E$  is in MeV;  $dE/dx$  is in  $\text{MeV g}^{-1}\text{cm}^2$ ;  $W_{bb}$  and  $W_v$ , the energy densities in black-body and starlight photons, are in  $\text{eV cm}^{-3}$ ; and  $f(E)$  is given by

$$f(E) = \begin{cases} 1; E < 4 \text{ GeV} \\ 1.6 E^{-0.3}; 4 \leq E \leq 80 \text{ GeV} \\ 308 E^{-1.5}; 80 \leq E \leq 800 \text{ GeV} \\ 2400 E^{-2} [\ln(0.025E) + 0.5]; E > 800 \text{ GeV.} \end{cases} \quad (7)$$

In the subsequent calculations we shall evaluate the total energy loss rate

$$\frac{dE}{dx} = \left(\frac{dE}{dx}\right)_{I+B} + \left(\frac{dE}{dx}\right)_s + \left(\frac{dE}{dx}\right)_c \quad (8)$$

in both neutral and ionized media for 4 cases defined as follows.

Case I:  $n_H = 1 \text{ cm}^{-3}$ ,  $B_{\perp} = B_0 = 4 \times 10^{-6} \text{ gauss}$

Case II:  $n_H = 0.1 \text{ cm}^{-3}$ ,  $B_{\perp} = B_0 \sqrt{n_H}$

Case III:  $n_H = 0.1 \text{ cm}^{-3}$ ,  $B_{\perp} = B_0$

Case IV:  $n_H = 5 \text{ cm}^{-3}$ ,  $B_{\perp} = B_0 \sqrt{n_H}$ .

Case I corresponds to cosmic-ray propagation in a medium of average density similar to that determined by 21 cm surveys. In case II cosmic rays propagate in a low-density medium which has the same  $B^2/n_H$  ratio as case I. Case III is for a low-density medium with the same magnetic field as case I. Case IV represents conditions which might be applicable for regions dominated by molecular clouds with a  $B^2/n_H$  ratio as in case I and II.

We have evaluated equations (1) and (2) with  $dE/dx$  given by equation (8) for neutral and ionized ambient media. The results are shown in Figure 2 for cases I, II, and III, together with the available positron data (Fanselow et al. 1969; Beuermann et al. 1969; Hartman and Pellerin 1976; Daugherty et al. 1975; Buffington et al. 1975). We shall discuss separately the results of case IV in connection with gamma-ray production in a dense interstellar medium.

We first consider our results for the closed-galaxy model. As can be seen, at low energies ( $E \leq 1 \text{ GeV}$ ), the calculated positron intensity is the same for cases I, II and III, i.e. it is independent of the assumed density and magnetic field of the interstellar medium. It depends, however, on the state of ionization of this medium. These

results follow because at low energies synchrotron and Compton losses are small, and the energy loss is mostly due to Coulomb and bremsstrahlung losses. These losses scale as  $n_H$  and are larger for an ionized ambient medium than for a neutral one. The production rate of positrons also scales as  $n_H$ , but is independent of the ionization state. Therefore, the positron intensity is independent of  $n_H$ , and decreases as the ratio of ions-to-neutrals increases.

At high energies ( $\gtrsim 1$  GeV), the calculated positron intensity depends on the density and magnetic field of the interstellar medium, but becomes quite insensitive to its state of ionization. The largest positron intensity is obtained in case I, which has the largest  $n_H/B_{\perp}^2$  ratio. The smallest intensity is found for case III, and an intermediate intensity is obtained for case II ( $n_H = 0.1 \text{ cm}^{-3}$  and  $B_{\perp} = 1.3 \times 10^{-6}$  gauss).

We do not show the positron intensity for case IV, since it is only somewhat larger than that for case I. As we shall discuss below, case I already gives an excessively large positron intensity, and hence both these cases cannot apply to the locally observed cosmic rays in the closed galaxy model. We shall discuss, however, this model in the context of galactic gamma-ray production in Section 5.

The interstellar positron intensity for the leaky-box model was calculated for an energy-dependent mean path length. In this model, such an energy dependence is implied by the observed variation with energy of the ratio of secondary-to-primary cosmic rays. We use the results of a recent analysis (Juliusson et al. 1975) which can be expressed as

$$\Lambda(E) = \begin{cases} 6 \text{ g cm}^{-2} & ; E \leq 3 \text{ GeV} \\ 6(E/3)^{-0.49} & ; E \geq 3 \text{ GeV} \end{cases} \quad (9)$$

The resultant intensity for the  $dE/dx$  of case I, neutral is shown in Figure 2. In the following, we shall use only this  $dE/dx$  for calculations in the leaky-box model.

Let us compare now the calculated interstellar positron intensities with data obtained near Earth. For all models, the calculated curves in Figure 2 below 1 GeV are much higher than the observations. This difference is most likely due to solar modulation. However, because there is no accurate independent information on the magnitude of the modulation, the results of this energy region cannot be used to differentiate between the models. In fact, in previous studies the magnitude of the modulation has been deduced by comparing the calculated and observed positron fluxes (Ramaty and Lingenfelter 1968; Cummings et al. 1973).

At energies above  $\sim 1$  GeV, however, the calculated positron intensities for the closed-galaxy model lie significantly above the observations, whereas the intensity for the leaky-box model does not. In particular, the intensity of case I is very probably too high. For example, it is unlikely that at 5 GeV solar modulation can reduce the interstellar intensity by as much as a factor of 5. On the other hand, we see no conflict between the interstellar intensities of cases II and III and the observed positron data. For case II, the magnitude of the necessary amount of modulation is about 2.5 at 5 GeV, and  $\sim 6$  at 1 GeV; for case III we need even less modulation. We note that a positron modulating factor of  $\sim 2.5$  at 5 GeV possibly implies a larger interstellar proton intensity than

that used in calculating the positron source function of Figure 1. This increase, however, has no effect on  $\sim 5$  GeV positron production, since these positrons are produced by  $\sim 10^3$  GeV protons which are very likely not affected by modulation. On the other hand, if the proton flux in the several GeV region is larger than that observed near Earth, the source function of low-energy ( $\leq 1$  GeV) positrons becomes greater than that shown in Figure 1. We discuss the implications of this effect in Section 5.

The average density of the medium through which cosmic rays propagate is  $1 \text{ cm}^{-3}$  for case I, and  $0.1 \text{ cm}^{-3}$  for cases II and III. The above results imply, therefore, that the closed-galaxy model is consistent with the positron data provided that the density in the confinement volume is of the order 0.1 or less. Such low densities are relevant, for example, if cosmic rays propagate through interstellar tunnels (Cox and Smith 1974) as proposed recently by Scott (1975). The densities in these tunnels are quite low, of the order  $0.01 \text{ cm}^{-3}$ . However, since the main feature of the closed-galaxy model is that cosmic rays are destroyed by interactions with the medium, the cosmic rays should not spend their entire lifetime in tunnels. For a density of  $0.01 \text{ cm}^{-3}$ , the average time between nuclear interactions for protons is  $5 \times 10^9$  years; it is unlikely that the cosmic rays are trapped in low density regions for times comparable to the age of the galaxy.

Using (1) and (2) with  $q_+$  replaced by  $q$  shown in Figure 1, we have also evaluated the interstellar flux of secondary electrons. The

results are shown in Figure 3 for a neutral interstellar medium. We have used the  $dE/dx$  of cases I, II, and IV for the closed galaxy, and  $dE/dx$  of case I, for the leaky-box model. We shall discuss the implications of these intensities in the next two sections.

#### 4. Interstellar Electron Intensities.

Because positrons and negatrons are expected to undergo the same solar modulation, the interstellar electron intensity,  $\phi(E)$ , can be obtained from the calculated positron intensity and measured positron-to-electron ratios. We have that

$$\phi(E) = \phi_+(E)/R(e^+/e), \quad (10)$$

where  $\phi_+(E)$  is the interstellar positron intensity as calculated in section 3, and  $R(e^+/e)$  is a fit to the measured  $e^+/e$  ratio.

Measurements of this ratio (see Buffington et al., 1975) are plotted in Figure 4 together with our assumed fit shown by the solid line. Since the ratio  $R(e^+/e)$  is energy dependent, equation (10) is valid only if cosmic rays do not lose energy during their penetration into the solar cavity. While the energy loss during modulation is quite large for nuclei (Goldstein, Fisk and Ramaty 1970), electrons around 1 GeV lose only about 10% to 20% of their energy (R. Hartman, private communication 1976).

We have evaluated equation (10) for all the positron intensities of Figure 2. We have assumed that the  $R(e^+/e)$  is constant both below 0.1 GeV and above 10 GeV, because there is no positron data in these energy ranges. This assumption for  $E > 10$  GeV is essentially equivalent to a choice of an electron source spectrum which has the same spectral index as the observed proton spectrum, because at these energies the

spectral index of the positron source,  $q_+(E)$ , is almost the same as that of its parent protons (Figure 1). At energies below 0.1 GeV a constant  $R = 0.3$  is consistent with the upper limits on the positron intensity measured in this energy region.

The results are shown in Figure 5. As in Figures 1 and 2, below 1 GeV we plot  $\phi(E)$ , while above this energy we plot  $E^{2.75}\phi(E)$ . As can be seen, at energies greater than a few GeV all spectra are steeper than the proton spectrum,  $E^{-2.75}$ . In the energy range from 10 to 100 GeV, the calculated spectral indexes are 3.45 and 3.6 for the closed galaxy in cases II and III, respectively, and 3.2 for the leaky-box model. In the closed galaxy, the steepening is due to the effects of the synchrotron and Compton losses. For the leaky box most of the steepening is due to energy dependent escape. As has been shown by Silverberg and Ramaty (1973), when  $\Lambda$  is energy dependent, the effects of the energy losses on the electron spectrum are diminished. As can be seen from their figure 1, for  $\Lambda \sim E^{-0.5}$ , the energy losses steepen the electron spectrum by only 0.05 in the energy range from 10 to 100 GeV. Thus, since we have assumed that the source spectrum of electrons is the same in this energy region as that of positrons ( $\sim 2.65$ , from Figure 1), the interstellar electron intensity should have a spectral index of  $2.65 + 0.49 + 0.05 \approx 3.2$ , just as we have found in the present paper. However, if the source spectrum of protons in the leaky-box model is  $2.75 - 0.49 = 2.26$ , as would be implied by an energy dependent escape lifetime given by equation (9), and if we assume that the electron source spectrum is the same as that of protons, the interstellar electron intensity has a

source spectrum of only  $2.26 + 0.49 + 0.05 = 2.8$ .

We thus find spectral indexes for  $10 \leq E \leq 100$  GeV ranging from 3.4 to 3.6 for the closed-galaxy model, and from 2.8 to 3.2 in the leaky-box model. The experimental data, however, cannot distinguish between these values. The spectral index was found to be  $3.4 \pm 0.1$  in the range  $6 \leq E \leq 100$  GeV (Meegan and Earl 1975),  $3.0 \pm 0.2$  in the range  $8 \leq E \leq 40$  GeV (Freier, Gilman and Waddington 1975), and  $3.1 \pm 0.08$  in the range  $10 \leq E \leq 200$  GeV (Silverberg 1976), and  $2.66 \pm 0.1$  in the range  $30 \leq E \leq 250$  GeV (Miller and Meyer 1973). We conclude that for the closed-galaxy model, case II is consistent with the data, while case III may yield an electron spectrum which is steeper than that observed.

To further investigate the consistency of the closed-galaxy case II with data, we have plotted in Figure 6 the measured electron intensities in the energy range from 10 GeV to about 700 GeV (Miller and Meyer 1973; Meegan and Earl 1975; Freier et al., 1975; Silverberg 1976; Matsuo et al., 1975) together with the calculated intensities for this model and the leaky-box model. The general tendency of the closed-galaxy curve is to steepen at high energies; the data points, on the other hand, do not show this trend. However, because the error bars and the scatter of the data are quite large, it is not possible to conclude that there is a discrepancy between this model and the data. Nevertheless, if future electron measurements at energies greater than  $\sim 10^3$  GeV would fall well above the calculated curve for the closed galaxy, the conclusion would be that a major fraction of the high-energy electrons come from nearby sources. This conclusion is consistent with the

property of the closed-galaxy model discussed in the Introduction, namely that such sources are necessary for the explanation of the observed cosmic-ray composition in this model. It should be noted, however, that even if all the observed high-energy electron intensity ( $> 200$  GeV) is from nearby sources, these sources contribute only a small fraction of the electron intensity at lower energies. Thus, for  $E^{2.75}\phi = 30$  electrons  $m^{-2}s^{-1}sr^{-1}$   $GeV^{1.75}$ , a value equal to the total flux at  $E > 200$  GeV, a spectral index of 2.75 implies that the local sources contribute in the few GeV region about 10% of the electron intensity of the closed galaxy model case II.

##### 5. Gamma Radiation.

In the closed-galaxy model, the interstellar electron intensity is in general greater than that in the leaky-box model. Therefore, the electromagnetic radiations due to bremsstrahlung and Compton scattering from these electrons are also enhanced. We proceed now to evaluate these radiations.

The bremsstrahlung emissivity per hydrogen atom from an electron intensity,  $\phi$ , can be written as (Ginzburg and Syrovatskii 1964 eq. 19.11)

$$q_B(>\epsilon) = 4.4 \times 10^{-25} \int_{\epsilon}^{\infty} d\epsilon \phi(>\epsilon)/\epsilon, \quad (11)$$

where  $q_B(>\epsilon)$  is the number of gamma rays of energies greater than  $\epsilon$  produced per second and per H (atom), and  $\phi(>\epsilon)$  is the intensity of electrons of energies greater than  $\epsilon$ , measured in particles  $cm^{-2}s^{-1}sr^{-1}$ . Equation (11) takes into account the contributions of atomic

electrons and heavy nuclei, and is valid in a neutral medium. In an ionised medium, the bremsstrahlung cross section is somewhat larger (Koch and Motz 1959), but this increase is compensated by the lower electron intensities in such a medium. We calculate, therefore, the bremsstrahlung emissivities in neutral media only. The results, however, are approximately valid also for the ionised cases.

In Table 1 we show the bremsstrahlung emissivities  $q_B (> 30 \text{ MeV})$  and  $q_B (> 100 \text{ MeV})$  for several of the models considered above. We also show the corresponding  $\pi^0$ -decay emissivities (Stecker 1971). It has been generally assumed that  $\pi^0$  decay is the dominant emission mechanism at energies greater than 100 MeV. As can be seen from Table 1, however, for the closed-galaxy model this assumption is, in general, not valid. For case II, which is consistent with the local positron and electron data, the bremsstrahlung emissivity at  $\epsilon > 100 \text{ MeV}$  is about equal to the  $\pi^0$ -decay emissivity, and it is larger by about 80% at  $\epsilon > 30 \text{ MeV}$ . In comparison, in the leaky-box model the bremsstrahlung emissivities for both  $\epsilon > 100 \text{ MeV}$  and  $\epsilon > 30 \text{ MeV}$  are less than 50% of the corresponding  $\pi^0$ -decay emissivities.

Observationally, gamma rays from bremsstrahlung and  $\pi^0$  decay can be distinguished by measuring the energy spectrum of the photons. In Table 1 we show the ratios  $[q_B (> 30 \text{ MeV}) + q_{\pi^0} (> 30 \text{ MeV})]/[q_B (> 100 \text{ MeV}) + q_{\pi^0} (> 100 \text{ MeV})]$  for the various models. We see that for the closed-galaxy models, this ratio is larger than for the leaky-box model. According to Fichtel et al. (1975), the measured value of the ratio of the gamma-ray flux above 30 MeV to the flux above 100 MeV is  $2 \pm 0.5$ . This result seems to favor the closed-galaxy models or any model with a larger low-energy electron

population than obtained for the leaky-box model in this paper. It should be noted that the interstellar electron intensity that we have deduced for all models at energies below  $\sim 100$  MeV are lower limits because we used upper limits on the  $e^+/e$  ratio in this energy region.

In the closed-galaxy model I bremsstrahlung is the dominant gamma-ray production mechanism, including the energy region above 100 MeV. As discussed in Section 3, this model is not consistent with the local positron data because it produces an interstellar positron flux which is larger than that observed, or that which can be extrapolated to interstellar space by a reasonable modulation. These constraints, however, do not apply to the principal gamma-ray producing regions of our Galaxy which lie at distances of at least several kpc from the solar system. (Bignami et al., 1975; Stecker et al., 1975).

It is, nevertheless, of considerable interest to ask whether the  $q_B$ 's of the closed-galaxy model case I are reasonable estimates of the bremsstrahlung emissivities of galactic gamma rays. These  $q_B$ 's are based on the assumption that the positron-electron ratio,  $R(e^+/e)$ , has the same value everywhere in the Galaxy as measured near Earth, even though the positron-proton ratio in case I is larger than observed near Earth. Another, perhaps more reasonable assumption would be that the ratio of primary negatrons to protons is the same everywhere in the galaxy. In this case we use the fact that the bremsstrahlung emissivity per hydrogen atom equals the local emissivity of primary electrons, plus the emissivity from secondary electrons. The latter quantities, based on the intensities given in Figure 3, are also given in Table 1 for the closed-galaxy model

cases I, II, III and IV, and for the leaky-box model. The parameters of case IV,  $n_H = 5 \text{ cm}^{-3}$  and  $B^2 \propto n_H$ , represent conditions which might be applicable for regions where the ambient density is dominated by dense molecular clouds.

The results are shown in Table 1. The local primary electrons are those of the closed-galaxy case I, for  $(IV)_s + (CGII)_p$ , and of the leaky-box, for  $(IV)_s + (LB)_p$ . In both cases the secondary electrons are obtained from the closed-galaxy model case IV. As can be seen, the resultant emissivities are only slightly larger than those for the closed-galaxy model II, but significantly in excess of those of the leaky-box model.

As we have mentioned in Section 3, the positron source function shown in Figure 1 has been calculated by using the solar minimum proton intensity. If the magnitude of the solar modulation for protons is as large as it is for positrons in case II, the positron production below  $\sim 1 \text{ GeV}$  becomes larger than given in Figure 1. Such an increase leads to larger bremsstrahlung and  $\pi^0$ -decay emissivities than those shown in Table 1. The ratio between these larger emissivities, however, is not expected to differ by much from those implied by the results of Table 1.

The contribution of Compton scattering to galactic gamma-ray production was analyzed by Shukla et al. (1975). These authors have used a local electron intensity of the form  $\phi(E) = 200E^{-2.95} (\text{electrons m}^{-2} \text{s}^{-1} \text{sr}^{-1} \text{GeV}^{-1})$  for energies greater than  $1 \text{ GeV}$ . They used various models for the distribution of visible, UV and  $I_{\alpha}$  photons in the galaxy, and they assumed

that the cosmic-ray electron intensity is proportional to the interstellar gas density. Their results indicate that Compton scattering is not an important mechanism for gamma-ray production at photon energies greater than 100 MeV. In particular, the gamma-ray flux from Compton scattering is lower than that observed from the direction of the galactic center by about a factor of 10.

The cosmic-ray electrons which are responsible for Compton gamma-ray production above  $\sim 100$  MeV have energies in the range from about 1 GeV to several hundred GeV: This gamma-ray energy range is populated by starlight photons scattered from electrons of several GeV, and by 3K black-body photons which have interacted with electrons of energies greater than  $\sim 200$  GeV.

If we compare the electron intensity used by Shukla et al. (1975) with the closed-galaxy case II spectrum shown in Figure 5, we find that the Shukla et al. spectrum is smaller by about a factor of 2 at 1 GeV, and that it is larger by  $\sim 2$  at 100 GeV. The resultant gamma-ray production by Compton scattering of electrons in the closed-galaxy II is, therefore, of about the same magnitude as that calculated by Shukla et al., and hence small in comparison with that observed from the direction of the galactic center.

## 6. SUMMARY.

We have calculated the interstellar intensities of cosmic-ray positrons and electrons in a model in which cosmic rays are lost due to interactions with the ambient medium before they can escape from the Galaxy. We refer to this model as the closed-galaxy model. We have

also evaluated the positron and electron intensities for the more commonly used leaky-box model in which cosmic rays can escape from the galaxy. For this model we have used an energy dependent mean escape length. We have then calculated the gamma-ray emissions due to bremsstrahlung and Compton scattering of the electrons in the various models.

A previous analysis of the nucleonic component of the cosmic rays (Rasmussen and Peters 1975) has shown that for the closed-galaxy model to be valid, major fractions of the locally observed primordial cosmic rays with  $Z \geq 2$  have to be from local sources. (The observed nuclei from these sources have not yet fully interacted with the interstellar medium.) Our analysis of cosmic-ray positrons, on the other hand, indicates that a similar constraint cannot be placed on protons. We find that a cosmic-ray proton intensity equal to that observed locally could exist throughout the confinement volume of the cosmic rays and produce a positron intensity consistent with observations, provided that the average density of the interstellar medium sampled by the cosmic rays is of the order  $0.1 \text{ cm}^{-3}$  or less. For larger densities the interstellar positron intensity is larger than that observed, or larger than the intensity extrapolated to interstellar space by a reasonable solar modulation.

The principal observational consequences of the closed-galaxy model on electrons and gamma rays are:

The model yields steep electron spectra at high energies. In the energy range from 10 to 100 GeV the electron differential spectral index is about 3.4 or steeper, provided that the source spectral index

of the electrons is the same as that of the protons and that there is no significant contribution of nearby sources to the local electron intensity in this energy region. As discussed in the paper, an index of 3.4 is consistent with at least some of the data. A stringent test of the closed-galaxy model would come from the measurement of the spectrum of positrons in this energy region: an index smaller than 3.4 would very likely be inconsistent with the model.

The model leads to large bremsstrahlung emission in the gamma-ray region. For photon energies greater than 100 MeV the bremsstrahlung emissivity in the closed galaxy model is about equal to the emissivity from  $\pi^0$  decay. For energies greater than 30 MeV it is larger by almost a factor of 2. The energy spectrum of the gamma rays in the above ranges is considerably steeper for the closed galaxy than for the leaky-box model.

Acknowledgments

We would like to thank Professor B. Peters and Dr. I.L. Rasmussen for very stimulating discussions on the properties of the closed galaxy model, and to Dr. R.C. Hartman for carefully reading the manuscript.

REFERENCES

Abraham, P. B., Brunstein, K. A., and Cline, T. L.: 1966, Phys. Rev., 150, 1088.

Badhwar, G. D., Golden, R. L., Brown, M. L., and Lacy, J. L.: 1975, Astrophysics and Space Science, 37, 283.

Beuerman, K. P., Rice, C. J., Stone, E. C., and Vogt, R. E.: 1969, Phys. Rev. Letters, 22, 412.

Bignami, G. F., Fichtel, C. E., Kniffen, D. A., and Thompson, D. J.: 1975, Astrophys. J., 199, 54.

Buffington, A., Orth, C. D., and Smoot, G. F.: 1975, Astrophys. J., 199, 669.

Cox, D. P., and Smith, B. W.: 1974, Astrophys. J. Letters, 189, L105.

Cummings, A. C., Stone, E. C., and Vogt, R. E.: 1973, 13th Intl. Cosmic Rays Conference, Denver, Colorado, 1, 340.

Daniel, R. R., and Stephens, S. A.: 1970, Space Science Rev., 10, 599.

Daugherty, J. K., Hartman, R. C., and Schmidt, P. J. A.: 1975, Astrophys. J., 198, 493.

Fanselow, J. L., Hartman, R. C., Hildebrand, R. H., and Meyer, P.: 1969, Astrophys. J., 158, 771.

Fichtel, C. E., Hartman, R. C., Kniffen, D. A., Thompson, D. J., Bignami, G. F., Ögelman, H., Özel, M. E., and Tümer, T.: 1975, Astrophys. J., 198, 163.

Freier, P., Gilman, C., and Waddington, C. J.: 1975, 14th Intl. Cosmic Ray Conf., Munich, Germany, 1, 425.

Ginzburg, V. L., and Syrovatskii, S. I.: 1964, The Origin of Cosmic Rays, McMillan, New York.

Goldstein, M. L., Fisk, L. A., and Ramaty, R.: 1970, Phys. Rev. Letters, 25, 832.

Hartman, R. C., and Pellerin, C.: 1976, Astrophys. J., in press.

Juliussen, E., Cesarsky, C. J., Meneguzzi, M., and Casse, M.: 1975, 14th Intl. Cosmic Ray Conference, Munich, Germany, 2, 653.

Koch, H. W. and Motz, J. W.: 1959, Rev. Mod. Phys., 31, 920.

Matsuo, M., Nishimura, J., Kobayashi, T., Niu, K., and Aizu, E.: 1975, 13th Intl. Cosmic Ray Conference, 1, 431.

Meegan, C. A., and Earl, J. A.: 1975, 14th Intl. Cosmic Ray Conf., Munich, Germany, 1, 419.

Meyer, J. P.: 1971, Isotopic Composition of the Primary Cosmic Radiation, P. M. Dauber, Editor, Danish Space Research Institute, P. 235.

Müller, D. and Meyer, P.: 1973, Astrophys. J., 185, 841.

Orth, C. D., and Buffington, A.: 1976, Astrophys. J., in press.

Perola, G. C., Scarsi, L., and Sironi, G.: 1967, Nuovo Cimento, 52B, 455.

Ramaty, R., and Lingenfelter, R. E.: 1968, Phys. Rev. Letters, 20, 120.

Ramaty, R.: 1974, High Energy Particles and Quanta in Astrophysics, F. B. McDonald and C. E. Fichtel, Editors, MIT Press, p. 122.

Rasmussen, I. L., and Peters, B.: 1975, Nature, 258, 412.

Ryan, M. J., Ormes, J. F., and Balasubrahmanyan, V. K.: 1972, Phys. Rev. Letters, 28, 985.

Scott, J. C.: 1975, *Nature*, 258, 58.

Shukla, P. G., Casse, M., Cesarsky, C. J., and Paul, J.: 1975,  
14th Intl. Cosmic Ray Conference, Munich, Germany, 1, 65.

Silverberg, R. F., and Ramaty, R.: 1973, *Nature*, 243, 134.

Silverberg, R. F.: 1976, NASA/GSFC preprint X-661-75-218.

Stecker, F. W.: 1971, Cosmic Gamma Rays, Mono Book Corp., Baltimore,

Stecker, F. W., Solomon, P. M., Scoville, N. Z., and Ryter, C. E.: 1975,  
*Astrophys. J.*, 201, 90.

Wang, H. T., and Ramaty, R.: 1975, *Astrophys. J.*, 202, 532.

TABLE 1

GAMMA RAY EMISSIVITIES  $\left[ \times 10^{25} \text{ sec(H atom)} \right]$

	$q_B (>30 \text{ MeV})$	$q_B (>100 \text{ MeV})$	$q(>30)/q(>100)$
<b>Closed Galaxy</b>			
<b>Total Electrons</b>			
I	3	1.5	1.7
II	2.4	1.1	1.7
III	2.1	.9	1.7
<b>Secondary Electrons</b>			
IV	.7	.3	
I	.7	.3	
II	.6	.2	
III	.5	.15	
<b>Leaky Box</b>			
<b>Total Electrons I</b>	.6	.3	1.4
<b>Secondary Electrons I</b>	.12	.05	
$(IV)_s + (CGII)_p$	2.5	1.2	1.7
$(IV)_s + (LBI)_p$	1.2	.5	1.6
	$q_{\pi^0} (>30 \text{ MeV})$	$q_{\pi^0} (>100 \text{ MeV})$	
$\pi^0$ DECAY	1.3	1.1	

FIGURE CAPTIONS

Fig. 1 The source functions of positrons,  $q_+(E)$ , and secondary electrons (positrons and negatrons),  $q(E)$ . Above 1 GeV these functions are multiplied by  $E^{2.75}$ .

Fig. 2 Interstellar positron intensities and positron data near Earth. Above 1 GeV all quantities are multiplied by  $E^{2.75}$ . Cases I, II and III refer to parameters of the interstellar medium. I:  $n_H = 1 \text{ cm}^{-3}$ ,  $B_{\perp} = 4 \mu\text{G}$ ; II:  $n_H = 0.1 \text{ cm}^{-3}$ ,  $B_{\perp} = 1.3 \mu\text{G}$ ; III:  $n_H = 1 \text{ cm}^{-3}$ ,  $B_{\perp} = 4 \mu\text{G}$ . For the leaky box:  $n_H = 1 \text{ cm}^{-3}$ ,  $B_{\perp} = 4 \mu\text{G}$ . Solid line: neutral interstellar medium; dashed line: ionized interstellar medium.

Fig. 3 Secondary electron (positron and negatron) intensities in interstellar space. The parameters of cases I and II and the leaky box are defined in the text and in the caption of figure 2. Case IV:  $n_H = 5 \text{ cm}^{-3}$ ,  $B_{\perp} = 8.9 \mu\text{G}$ . The results of this figure are for a neutral interstellar medium.

Fig. 4 Measured  $e^+/e$  ratios and our assumed fit to these measurements.

Fig. 5 Total electron (positron, and primary and secondary negatron) intensities in interstellar space. The parameters are defined in the text and in the caption of figure 2.

Fig. 6      Interstellar electron intensities above 10 GeV. The  
closed-galaxy curve is for case II, neutral, and the leaky-  
box curve is for case I, neutral.

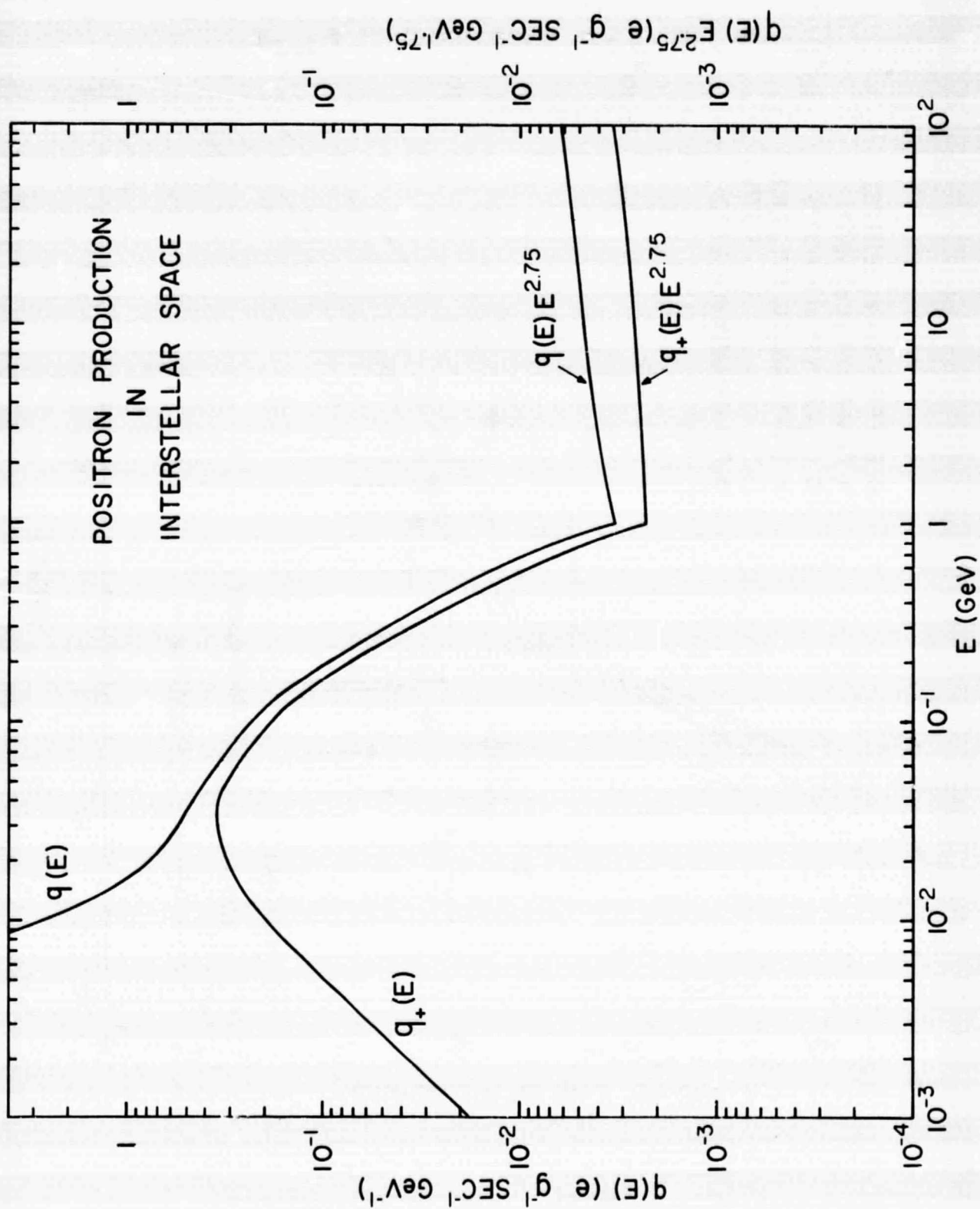


Figure 1

PRECEDING PAGE BLANK NOT FILMED

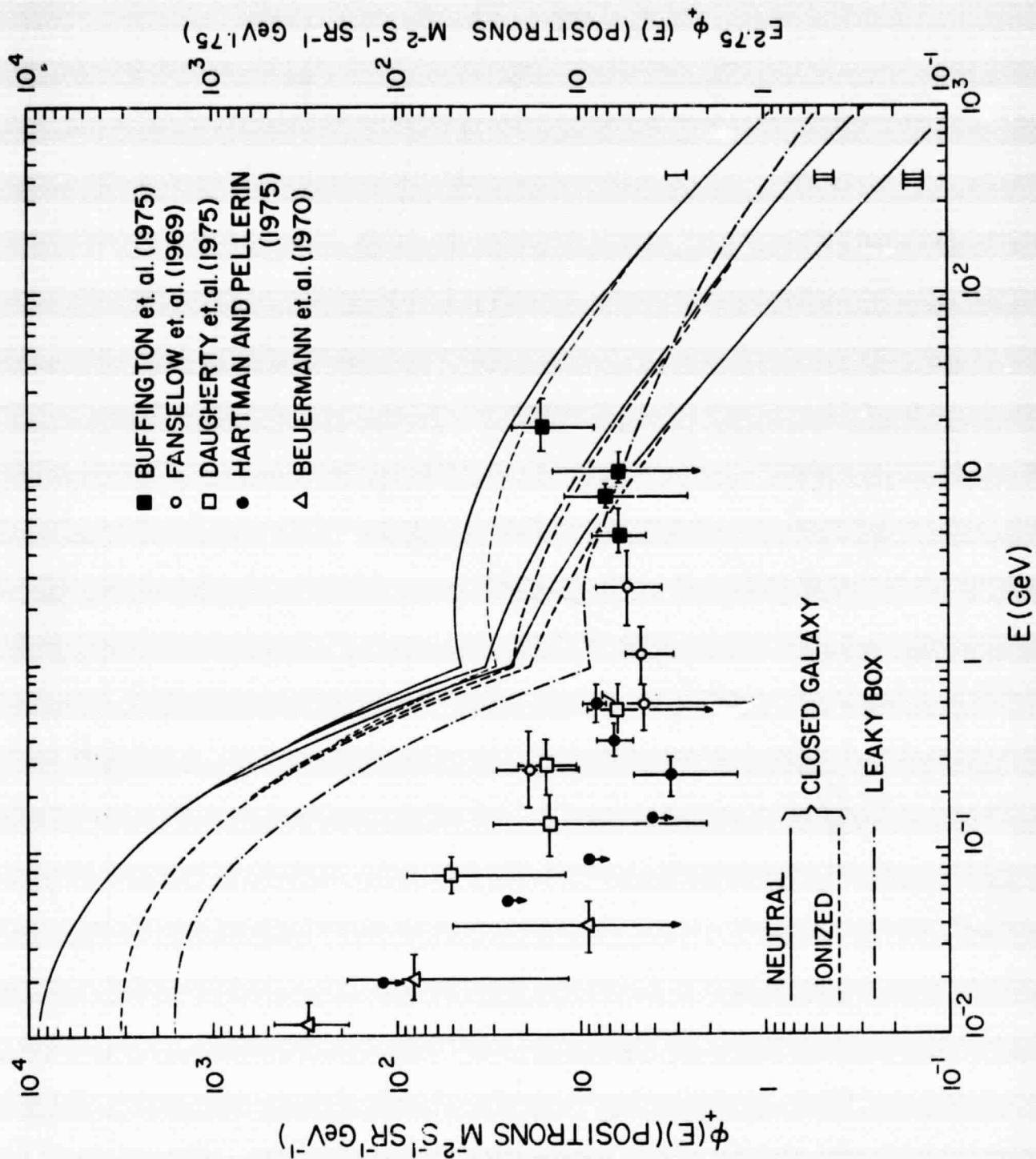


Figure 2

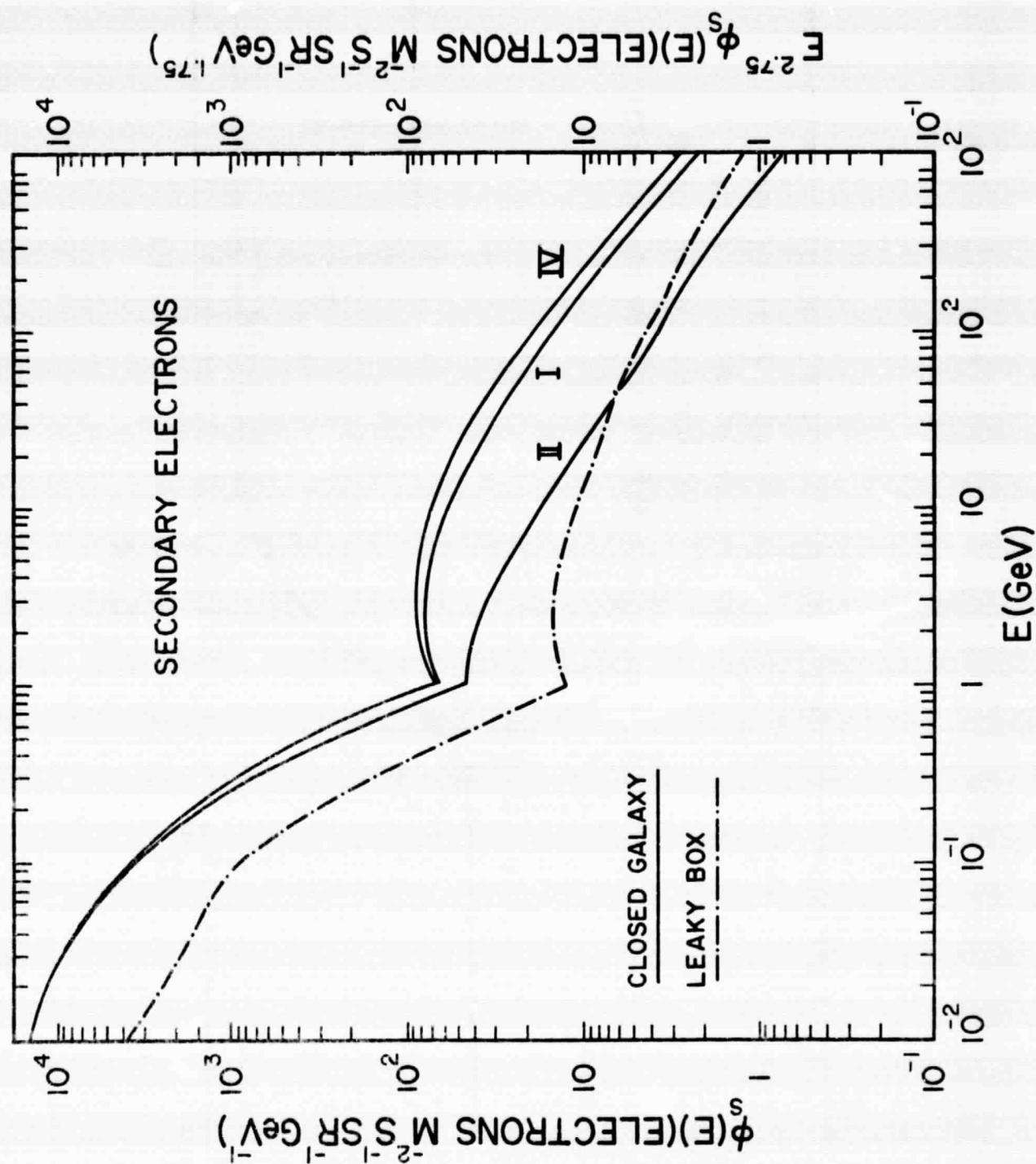


Figure 3

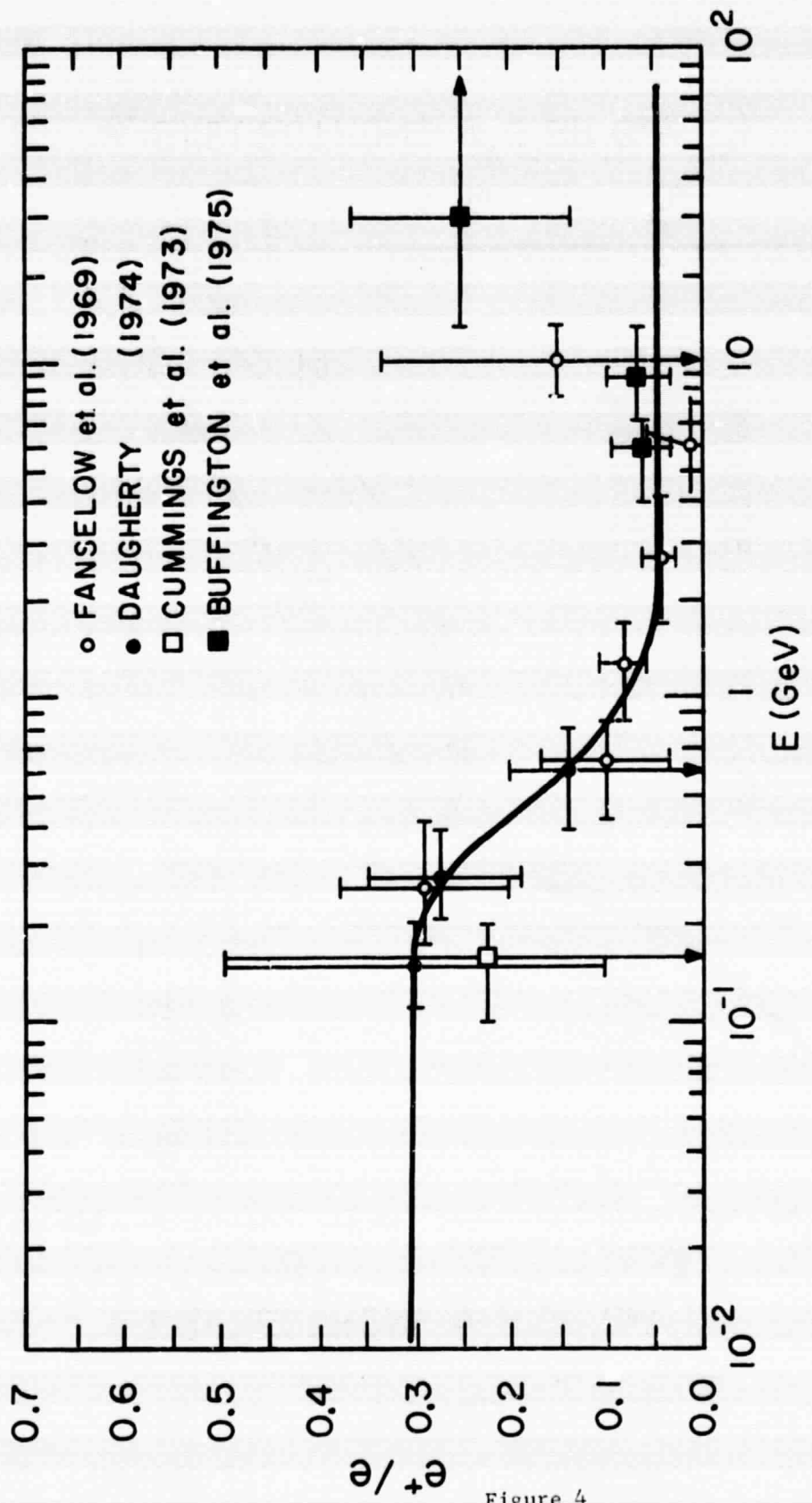


Figure 4

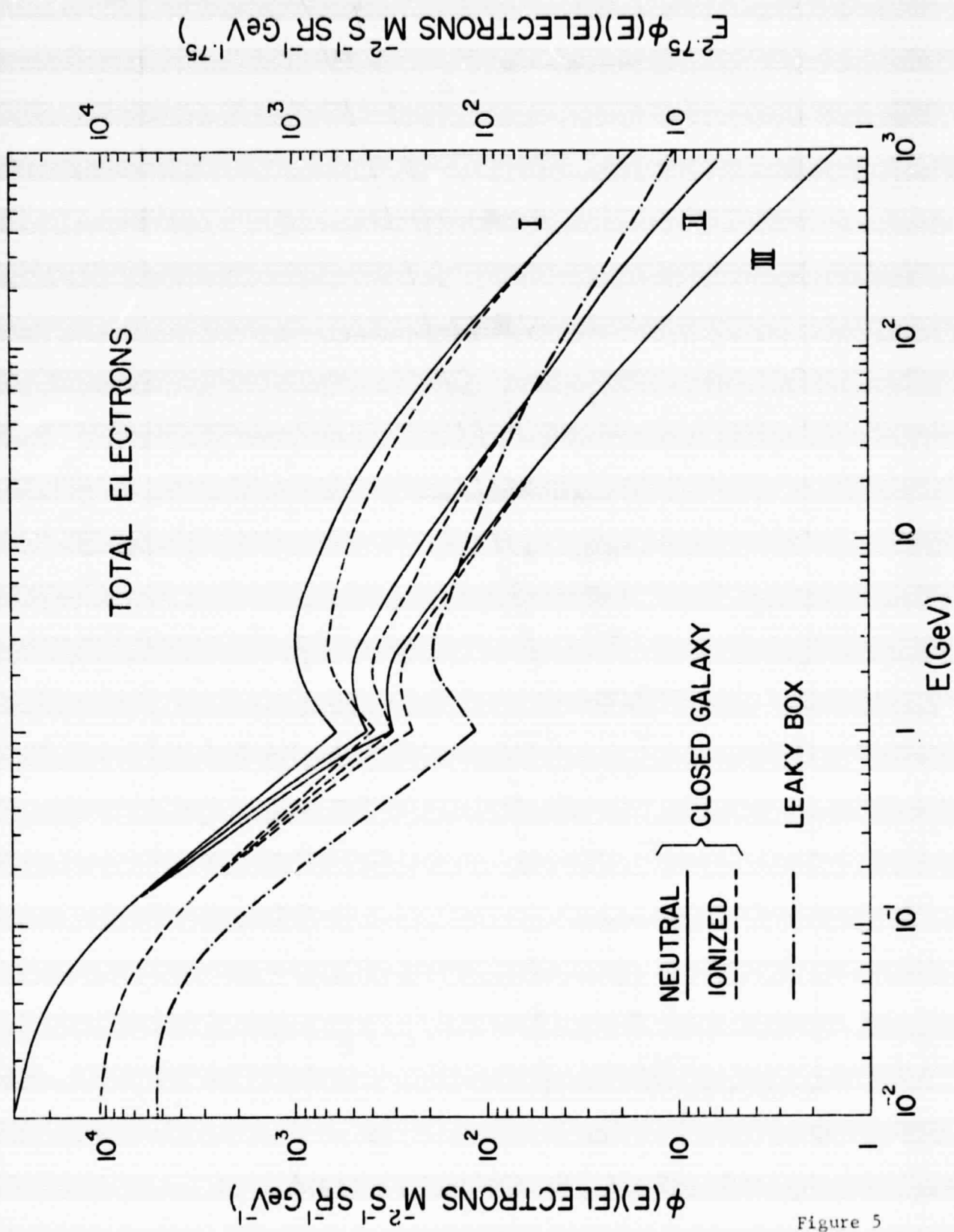


Figure 5

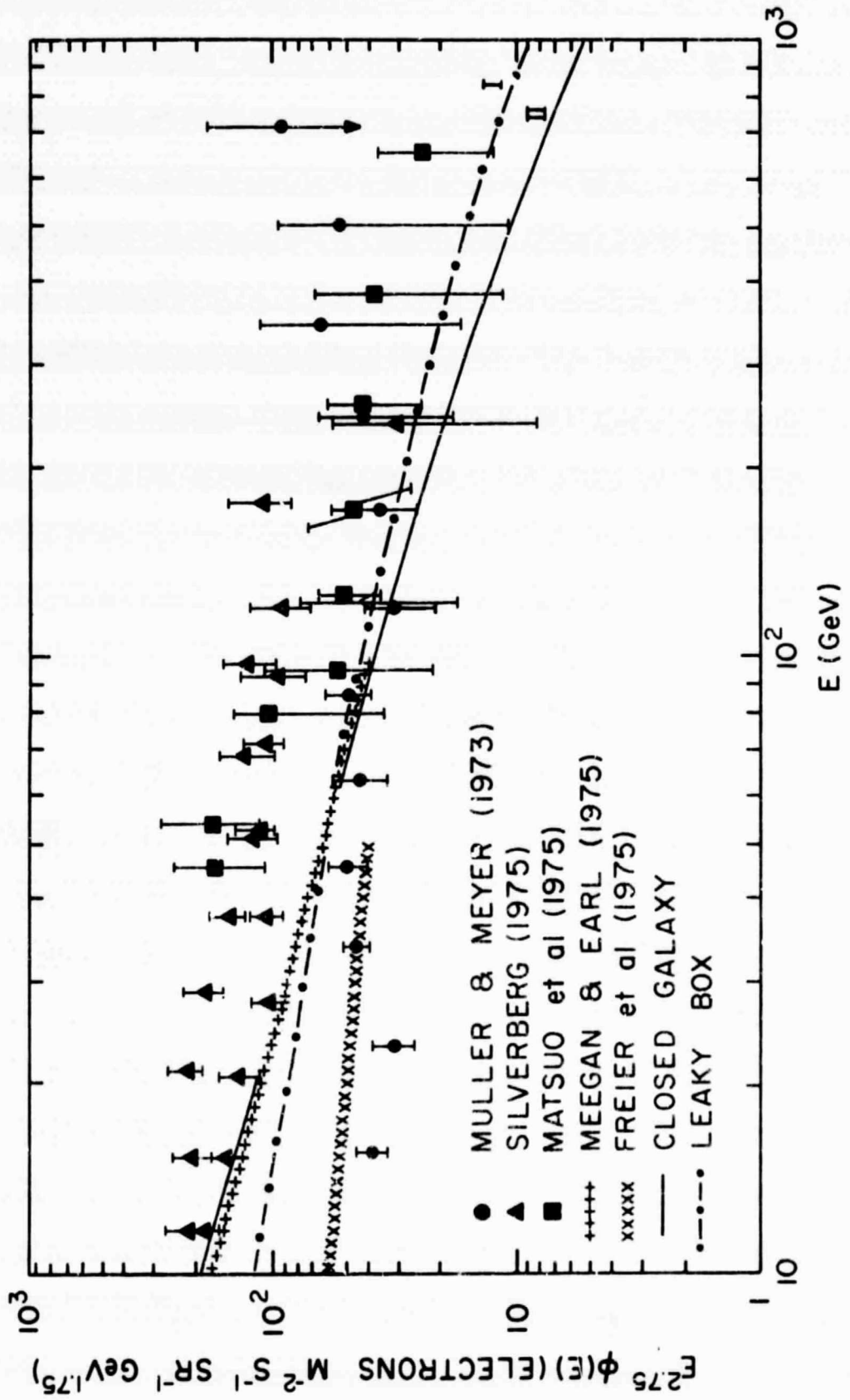


Figure 6